Title
Measuring Vertical Displacement Using Laser Lines and Cameras

Authors
Sinha, Sumeet Kumar
Kutter, Bruce Lloyd
Ziotopoulou, Katerina

International Journal of Physical Modelling in Geotechnics

ice Publishing

Measuring vertical displacement using laser lines and cameras

1 **Sumeet Kumar Sinha** MS
PhD candidate, Department of Civil and Environmental Engineering,
UC Davis, Davis, CA, USA (Orcid:0000-0002-2011-4887)
(corresponding author: sumeet.kumar507@gmail.com)

2 **Bruce Lloyd Kutter** PhD
Professor Emeritus, Department of Civil and Environmental
Engineering, UC Davis, Davis, CA, USA (Orcid:0000-0002-0628-1275)

3 **Katerina Ziotopoulou** PhD, PE
Assistant Professor, Department of Civil and Environmental
Engineering, UC Davis, Davis, CA, USA (Orcid:0000-0001-5494-497X)

Measuring displacements in model tests typically involves contact-based sensors such as linear potentiometers, where contact between two moving parts occurs at the sensing point. The sensor's finite mass, the limited stiffness of the beams and the clamping mechanism, and the slippage and hinging of the sensor body could affect the object's response and lead to measurement errors. Also, the physical mounting rack required to hold these sensors often obstructs the view and makes significant areas unavailable for conducting some other essential investigations. The advancement in high-speed, high-resolution and reasonably priced rugged cameras makes it feasible to obtain better displacement measurements by image analysis. This paper introduces a non-contact method that works by video recording the projection of laser lines on a test object to measure static and dynamic vertical displacements. The technique produces a continuous settlement distribution along the laser line passing through multiple objects of interest. This paper presents the theory for converting laser line images to displacements. The new method's validity is demonstrated by comparing the results from other measurement techniques: hand measurements, linear potentiometers and three-dimensional stereophotogrammetry.

Keywords: centrifuge modelling/model tests/settlement

Notation

α	slope of the settled test surface
Δu	actual horizontal movement of the laser line
Δu_c	recorded horizontal movement of the laser line by a camera
Δv	vertical movement of the test surface
$\Delta \phi$	change in the camera view angle from movement of the laser line
η	angle intersected at the test surface by the ray from the laser and camera
θ	measure of laser angle with respect to horizontal
ϕ	camera angle with respect to vertical

1. Introduction

Contact-based sensors such as linear potentiometers (LPs) or linear variable differential transformers (LVDTs) are commonly used to record relative displacements between the sensor's body and a probe attached to a test object in model tests. Figure 1 shows the typical set-up requirement for using linear displacement sensors. The sensor's body is clamped to a fixed support beam with its vertical sensing probe rested on an interface plate attached to the test object to enable smooth sliding in all three (x, y and z) dimensions. These sensors work well when the probe is firmly attached to the test object, the body of the sensor is effectively clamped to a stiff support reference frame and the test object is stiff and moves in a known direction. The benefits of these sensors include long measuring distance, target material insensitivity and lower cost. However, several problems occur while using these linear displacement sensors, especially while measuring dynamic displacements. First, the mass of the sensors and the limited stiffness of the beams and clamping mechanisms that hold the bodies of the LPs or LVDTs result in erroneous vibrations being superimposed on the quantity desired to be measured; this is especially problematic when the natural frequency of the
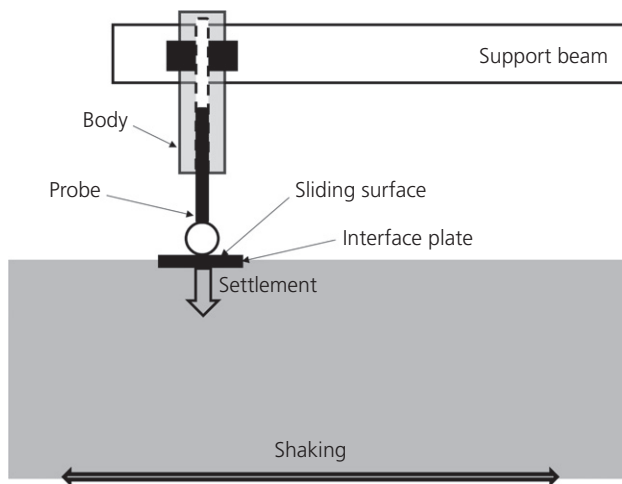
1

International Journal of Physical Modelling in Geotechnics

Measuring vertical displacement using
laser lines and cameras
Sinha, Kutter and Ziotopoulou

Figure 1. Typical system for measuring displacement of a soil surface using LPs

sensor support(s) is similar to the frequency of shaking in a dynamic experiment. Resonant vibration of the reference frame support, which is difficult to avoid during high-frequency shaking typical of dynamic centrifuge model tests, often makes dynamic measurements unreliable. Kutter and Balakrishnan (1998) described a method to filter and combine data from multiple displacements and accelerometer sensors to circumvent this problem and produce reliable dynamic displacement measurements. Second, the finite mass of the probes and the interface plate, and friction on the sliding surface shown in Figure 1, might affect the recorded displacement. For low-stiffness surfaces like soil during liquefaction, the sensors or the interface plate can reinforce soil and resist displacement (Fiegel and Kutter, 1994). Third, strong shaking or lateral displacement can cause the sensor to slip or even fall off the interface plate resulting in erroneous results or even no data recording. Other limitations regarding the use of LPs are the presence of a clamping mechanism and support beam that obstruct the model surface for video monitoring and make significant areas unavailable to conduct some other essential investigations. Also, as shown in Figure 1, the immense physical set-up requirement often limits its application to a small number of test objects.

Non-contact-based methods such as X-ray, particle image velocimetry (PIV), digital image correlation (DIC), laser displacement transducers and laser scanners offer an advantage over the contact-based sensors in obtaining measurements without affecting the dynamic response of the measured target. Gerber (1929) used the X-ray method to measure displacement within the soil. The technique used successive radiographs of lead shots embedded in the soil to get incremental movements.

The method successfully produced shear and volumetric strains with a precision of 0.1% (James, 1965). PIV uses image analysis techniques to examine the movement of small patches within an image (Adrian, 1991). White et al. (2001) used PIV to measure deformations in sand and clay and reported a precision in the order of 100 μm for a soil model having a patch size of 300 mm × 200 mm. DIC also uses image analysis of videos recorded from one or more cameras to obtain two-dimensional or three-dimensional (3D) movements of targets. Carey et al. (2018) used five cameras and soil surface markers to track dynamic and residual displacements of a submerged sloping liquefied ground using the software GEOPIV. Sinha et al. (2021c) used four high-speed cameras and the image analysis software TEMA (ISMA, 2019) to obtain 3D movements of the soil surface and a pile subject to shaking in liquefiable ground. The accuracy of measurements was reported to be 150 μm. These image analysis-based methods (PIV and DIC) are very effective and state of the art in obtaining continuous spatial and temporal 3D movements of a model. However, they can often get expensive in terms of the number of cameras, the processing time and the expertise required to analyse and process the images. Farrell (2010) and Ritter (2017) used laser transducers to measure movement at a point with high precision (5 μm). However, each sensor was relatively expensive, had a limited range of lateral motion and could only measure one point. Recently, commercial laser scanners have been used in centrifuge tests to obtain surface settlements (Ritter, 2017; Sinha et al., 2021b) over an area. The laser scanners provide a very detailed 3D surface of the model; however, they are also expensive and too slow to be used for dynamic measurements.

A new non-contact-based method is developed using image analysis of laser lines projected on a surface to determine static and dynamic vertical displacements. This method requires a high-speed camera to record the video and image processing to trace and process the laser lines. Having no physical contact eliminates the concern of changing the structural response and makes the model surface available for performing other important investigations. Since one laser line and one camera can cover many components of an experiment, the method can significantly reduce sensor requirements. The new method provides continuous displacement data distribution along the length of the laser line. The laser and camera can be mounted remote from the surface of interest, reducing congestion. The accuracy of the measurement produced is of the same order as that of DIC and PIV methods. However, the proposed method is relatively cheaper and has simpler and faster image processing techniques and analysis procedures than PIV and DIC methods.

This paper describes the instrumentation, image processing and theory for the new method, and presents results from two

2

International Journal of Physical Modelling in Geotechnics

Measuring vertical displacement using
laser lines and cameras
Sinha, Kutter and Ziotopoulou

recently conducted centrifuge model tests. The new method is validated by comparing results to those obtained by hand measurement, LPs and the 3D stereophotogrammetry method using a commercial software package.

2. Methodology

The concept behind using cameras and lasers to measure vertical movement is shown in Figure 2. The laser projects a plane of light at an angle (θ) from the horizontal, making a line on the surface. Undulations present on the surface will distort the straightness of the laser line. Vertical movement (Δv) of the surface results in recorded horizontal movement (Δu_c) of the laser line by the camera. For a vertically mounted camera, the vertical movement (Δv) of the surface can be obtained from measuring the laser line's horizontal movement (Δu_c), as $\Delta v = \Delta u_c \tan \theta$. Figure 2(b) shows the laser line's horizontal movement as recorded by the camera from the induced surface settlement after several shakings on the centrifuge model SKS02 (Sinha *et al.*, 2021a).

2.1 Formulation

Figure 3 shows the schematic diagram for a general case of camera angle (ϕ), laser angle (θ) and settled test surface with a sloping angle (α). The position of the laser, the camera and the laser line is initially measured to obtain the laser angle (θ) and the initial camera angle (ϕ). The camera angle (ϕ) measured from the vertical is the view angle it makes with the laser line on the initial position of the test surface. The angle (α) represents the slope of the final settled test surface with respect to the horizontal. Projecting the initial laser position to the final frame as recorded by the camera results in recorded horizontal movement Δu_c, while the actual horizontal movement is Δu.

From trigonometry, the vertical movement (Δv) is given as

1. $$\Delta v = \Delta u_c \frac{\cos \alpha - \sin \alpha \tan \phi}{1 + \tan \theta \tan \phi} (\tan \theta + \tan \alpha)$$

where Δv is the actual vertical movement of the test surface at the initial laser line position and Δu_c is the recorded horizontal movement of the laser line by the camera. The actual horizontal movement (Δu) of the laser line is given as

2. $$\Delta u = \Delta u_c \frac{\cos \alpha - \sin \alpha \tan \phi}{1 + \tan \theta \tan \phi}$$

Theoretically, for any configuration of laser angle (θ) and camera angle (ϕ) that results in non-zero recorded horizontal movement ($\Delta u_c \neq 0$) of laser lines, this method can be used to obtain vertical movements (Δv). The flexibility of choosing the camera and laser angles enables exposing the model surface area to carry out other important investigations. Some configurations of laser angle (θ), camera angle (ϕ) and settled test surface with sloping angle (α) are worth pointing out and are presented in the section below.

Case 1: levelled settled test surface, $\alpha = 0$

If the settled test surface is levelled (i.e. $\alpha = 0$), Equation 1 reduces to

3. $$\Delta v = \Delta u_c \frac{\tan \theta}{1 + \tan \theta \tan \phi}, \quad \Delta u = \Delta u_c \frac{1}{1 + \tan \theta \tan \phi}$$
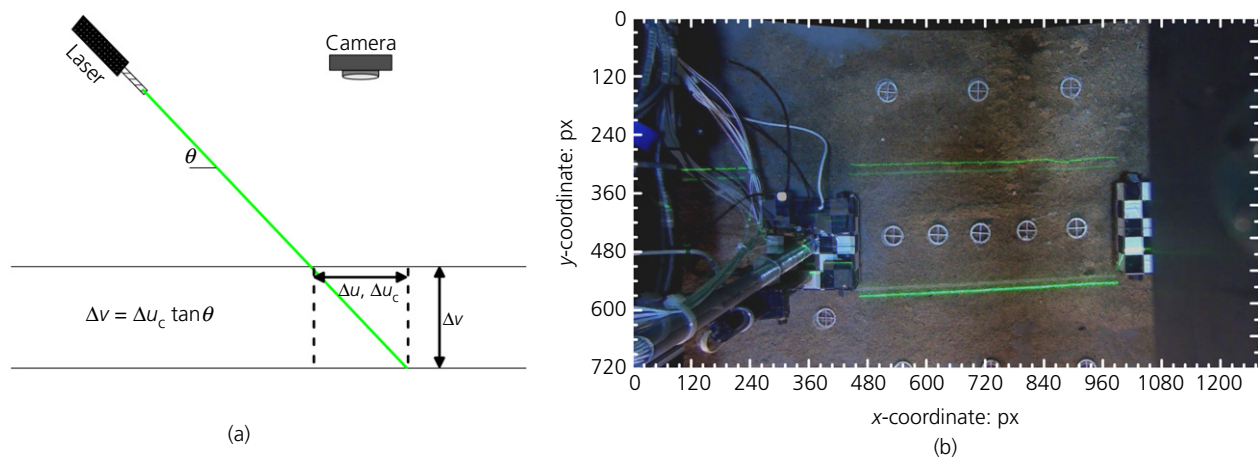

Figure 2. Schematic diagram showing the working of laser lines to measure vertical settlements: (a) methodology and (b) superposition of two images showing movement of the laser line due to settlement of the surface of the SKS02 (Section 3.1) centrifuge model test
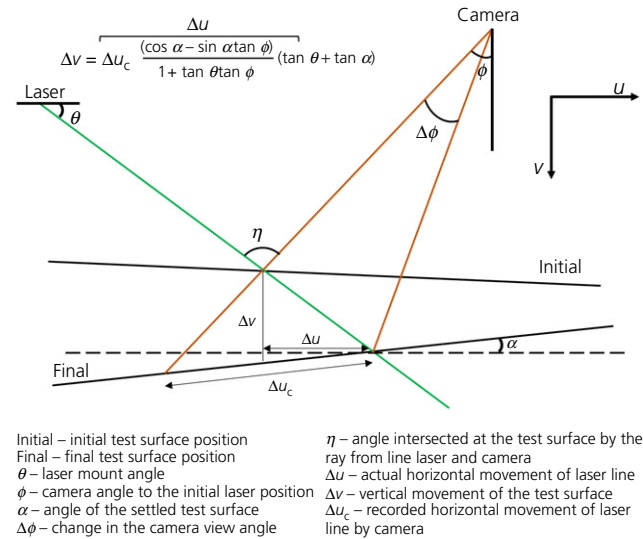
3

International Journal of Physical Modelling in Geotechnics

Measuring vertical displacement using
laser lines and cameras
Sinha, Kutter and Ziotopoulou

$$\Delta v = \Delta u_c \frac{(\cos \alpha - \sin \alpha \tan \phi)}{1 + \tan \theta \tan \phi} (\tan \theta + \tan \alpha)$$

Initial – initial test surface position
Final – final test surface position
θ – laser mount angle
ϕ – camera angle to the initial laser position
α – angle of the settled test surface
$\Delta \phi$ – change in the camera view angle

η – angle intersected at the test surface by the ray from line laser and camera
Δu – actual horizontal movement of laser line
Δv – vertical movement of the test surface
Δu_c – recorded horizontal movement of laser line by camera

Figure 3. Schematic diagram showing the movement of laser lines for laser angle θ, camera angle ϕ and angle of settled test surface with sloping ground (α)

In this case, the actual (Δu) and the recorded (Δu_c) horizontal movement of the laser lines occurs in the same plane. As a result, the vertical movement (Δv) can be expressed only in terms of the actual horizontal movement (Δu) of the laser line and laser angle (θ) as $\Delta v = \Delta u \tan \theta$.

Case 2: camera looking vertically down, $\phi = 0$ on a levelled settled surface, $\alpha = 0$

When the camera is looking vertically down on the laser line – that is, the camera angle is $\phi = 0$; on a levelled settled surface ($\alpha = 0$), Equation 1 reduces to

4. $\quad \Delta v = \Delta u_c \tan \theta, \quad \Delta u = \Delta u_c$

Figure 2(a) shows the case when the camera is vertical. In this case, the camera records the actual horizontal movement of the laser line (i.e. $\Delta u = \Delta u_c$).

Case 3: laser pointing vertically down, $\theta = \pi/2$ on a levelled settled surface, $\alpha = 0$

When the laser is projecting vertical downward ($\theta = \pi/2$) on the test surface on a levelled settled surface condition ($\alpha = 0$), Equation 1 reduces to

5. $\quad \Delta v = \Delta u_c \cot \theta, \quad \Delta u = 0$

In this case, although the laser line does not physically move horizontally ($\Delta u = 0$) with the movement of the test surface, the slant view angle (ϕ) of the camera can still record the horizontal movement ($\Delta u_c \neq 0$) of the laser line from which vertical movement (Δv) can be obtained.

2.2 Image processing to obtain horizontal movement (Δu_c)

The recorded video is processed frame by frame to trace the laser lines and obtain horizontal movements in pixels (Δpx). The camera is initially calibrated to correct the recorded videos for distortion and obtain the calibration factor ($f_{px,mm}$). The calibration factor ($f_{px,mm}$) is the extrinsic property representing the number of pixels per unit millimetre of the physical measurement of real-world objects in the image. For example, if a target marker of 10 mm diameter placed near the laser line occupies 20 pixels in the recorded image, the calibration factor ($f_{px,mm}$) would be 2 px/mm. Section 4.1 describes how edge detection of the markers placed in the model was used on the recorded images to obtain the spatially varying calibration factor ($f_{px,mm}$). With the calibration factor obtained, the recorded horizontal movement (Δu_c), as shown in Figure 2, is given as

6. $\quad \Delta u_c = \dfrac{\Delta px}{f_{px,mm}}$

The accuracy of tracing the laser lines depends on the resolution of the image. A subpixel accuracy of 0.25 px or higher can be achieved by analysing the red green blue (RGB) values of the pixels crossing the laser line. The resolution could be improved by using a higher-quality laser that produces a sharper laser line. An image with a higher resolution will produce a greater pixel density resulting in a larger calibration factor ($f_{px,mm}$). Placing the camera closer to the laser line will also produce greater pixel density, resulting in a higher calibration factor ($f_{px,mm}$). It can be seen from Equation 6 that as the calibration factor increases, the measurement accuracy of the horizontal movement of the laser line (Δu_c) also increases. Figure 4(a) shows the use of a smooth spline function $f(x)$ on RGB values of the pixels to identify the peak and hence the laser points' coordinates with subpixel accuracy of 0.1 px. For each y-coordinate, scanning was done in the x-direction to identify the laser position. Figure 4(b) shows the traced laser line on the image using the smooth spline interpolation algorithm.

2.3 Practical considerations

Equations 2 and 6 can be combined to obtain vertical movement (Δv) in terms of horizontal movement of laser line in pixels (Δpx) as

7. $\quad \Delta v = \Delta px \dfrac{1}{f_{px,mm}} \dfrac{\cos \alpha - \sin \alpha \tan \phi}{1 + \tan \theta \tan \phi} (\tan \theta + \tan \alpha)$

4

International Journal of Physical Modelling in Geotechnics

Measuring vertical displacement using
laser lines and cameras
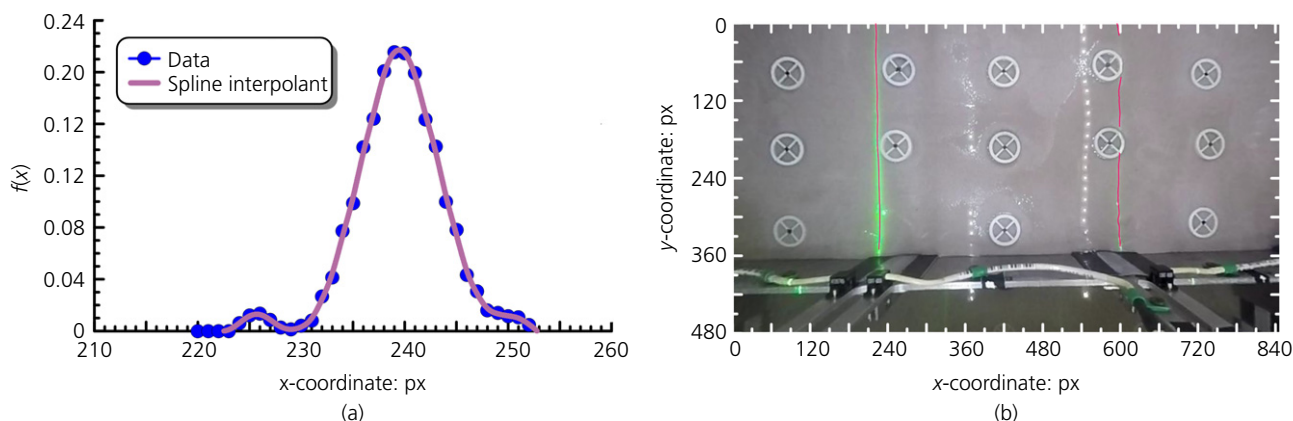Sinha, Kutter and Ziotopoulou

Figure 4. Image processing of a frame recorded by GoPro Hero3 from BLK01 (Section 3.2) centrifuge model test: (a) using smooth spline functions, (b) traced laser lines on the video frame

For a given laser angle (θ), camera angle (ϕ) and settled surface of the sloping angle (α), the resolution in the measured vertical movement (Δv) increases with the calibration factor ($f_{px,mm}$). Bringing the camera closer to the laser lines or increasing video recording resolution increases the calibration factor. The length of the laser line appearing in the images is controlled by the camera's view angle. A camera with a larger view angle will record a larger view of the model with longer laser lines. It must be noted that increasing the view angle is inversely related to magnification (or the calibration factor). A smaller view angle will generally produce a larger calibration factor resulting in greater precision over a shorter line. In such cases, multiple cameras can be used to view different parts of the model and processed separately to get settlements. Surface markers or rectangular grids of known size can be installed on the test surface near the laser lines (see Figure 4(b)) to obtain the calibration factor ($f_{px,mm}$) locally in space and time. For measuring dynamic movements, the camera should also have a sufficient frame rate. Ten frames per cycle of the frequency of interest produces very good resolution of peak displacements. It should be noted that the frame rate of the camera does not affect the accuracy of a displacement measurement as long as motion blurring is not an issue. The camera frame rate must be greater than the frequency of vibration to resolve the amplitude of cyclic displacements.

The laser and the camera should be rigidly mounted to a fixed frame to avoid measurement errors and changes in angles during dynamic motion. It is desired to pick the laser angle (θ) and camera angle (ϕ), which produces the most accurate indication of the vertical displacement (Δv), considering the resolution and uncertainties in the measurement of angle θ and ϕ. When the settled test surface is levelled (i.e. $\alpha = 0$), the sensitivity of the recorded horizontal movement of the laser line to the vertical movement ($\Delta px/\Delta v$) is given by

8.
$$\frac{\Delta px}{\Delta v} = f_{px,mm} \ (\cot \theta + \tan \phi)$$
$$= f_{px,mm} \ \tan \eta \ (1 - \tan (\eta - \phi) \tan \phi)$$

where $\eta = \pi/2 - \theta + \phi$ is the intersection angle made at the soil surface by the laser line and ray from the camera at view angle (ϕ) as shown in Figure 3. From symmetry, the distinct range of camera angle (ϕ) and laser angle (θ) varies between 0 and $\pi/2$. Thus, for a camera angle (ϕ), the intersection angle (η) can vary between ϕ and $\pi/2 + \phi$. From Equation 8, the sensitivity is minimum for $\eta = 0$ – that is, when the camera view angle and the laser are parallel. Maximum sensitivity is achieved when either the laser angle or the camera angle is horizontal – that is, for $\theta = 0$ or $\phi = \pi/2$. Alternatively, sensitivity increases with the increase in the intersection angle (η). However, with a large intersection angle η, even a small measurement error in laser angle ($\Delta\theta$) or camera angle ($\Delta\phi$) would propagate significant errors in recorded horizontal movement (Δu_c). Qualitatively, to achieve maximum sensitivity to vertical settlement and minimum sensitivity to angle measurement errors, the intersection angle (η) can be preferred to be in the middle – that is, close to $\eta = \pi/4 + \phi/2$.

Errors can also occur while processing laser lines from changes in lighting, obstruction from the moving of nearby objects, glare and reflections from water (or fluid). A contrasting background to laser line colour helps to make the tracing easier. Glare can be reduced by carefully placing the lighting source. The roughness of the test surface or change in the orientation of the particles can introduce apparent vertical movements. Higher is the roughness, and the size of particles, more

5

International Journal of Physical Modelling in Geotechnics

Measuring vertical displacement using
laser lines and cameras
Sinha, Kutter and Ziotopoulou

significant is the error introduced. The thickness of the laser line can limit the accuracy of tracing the laser lines. The methods described by the International Digital Image Correlation Society (IDICS *et al.*, 2018) and Sinha *et al.* (2021c) can be used as references for understanding the basic concepts of digital image correlation (DIC) and photography techniques used in testing. When testing surfaces submerged in water (or any fluid), reflection and refraction of the laser line at the interface can produce interesting effects. Refraction can result in the appearance of two laser lines, one on the water surface and another on the testing surface. The two laser lines can measure the movements of both the water and the testing surface beneath it. For a camera looking perpendicularly down on the laser lines ($\phi = 0$), increasing the laser angle θ (in the range of [0, $\pi/2$]), would decrease the separation distance

between the laser lines. However, the apparent separation distance between the laser lines can still be increased by increasing the camera angle (ϕ). For example, a laser pointing perpendicularly downwards ($\theta = \pi/2$) will result in no separation between the laser lines when viewed from the top (i.e. camera angle of $\phi = 0$). However, the lines can still be seen separated when viewed from the side (i.e. by increasing the camera angle $\phi > 0$). The larger the camera angle difference between the laser lines, the larger would be their separation distance. Reflection of the laser line at the interface can produce scattering and can increase laser line thickness, making its tracing difficult. In such cases, a laser pointing vertically downward (i.e. $\theta = \pi/2$) would be preferred to reduce scattering and produce sharp laser lines.

3. Application in centrifuge model tests

The new method was incorporated in two centrifuge tests SKS02 (Sinha *et al.*, 2021a) and BLK01, conducted on the 9 m radius large centrifuge testing facility at the Center for Geotechnical Modelling at the University of California, Davis.

3.1 SKS02 centrifuge test

The SKS02 centrifuge model test studied liquefaction-induced downdrag on axially loaded piles. Two piles were installed in a layered soil profile. The model was shaken with multiple small to large, scaled Santa Cruz (1989 Loma Prieta earthquake) motions (EQM_1–EQM_6) with peak ground acceleration (PGA) ranging from 0.01 to 0.4g. Two soil settlement markers, SM_1 and SM_2, were installed to measure the soil settlement at two different points in the model, as shown in Figure 6. Two LPs, $Pile_1^{LP}$ and $Pile_2^{LP}$, were installed to measure the settlement in piles. Additionally, hand measurements whenever possible
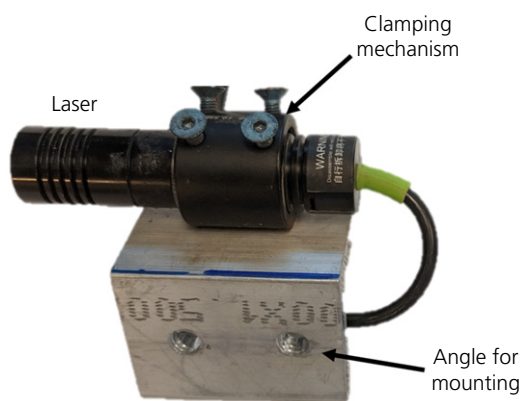
Figure 5. A view of the laser used in the experiment showing the clamping and mounting mechanism
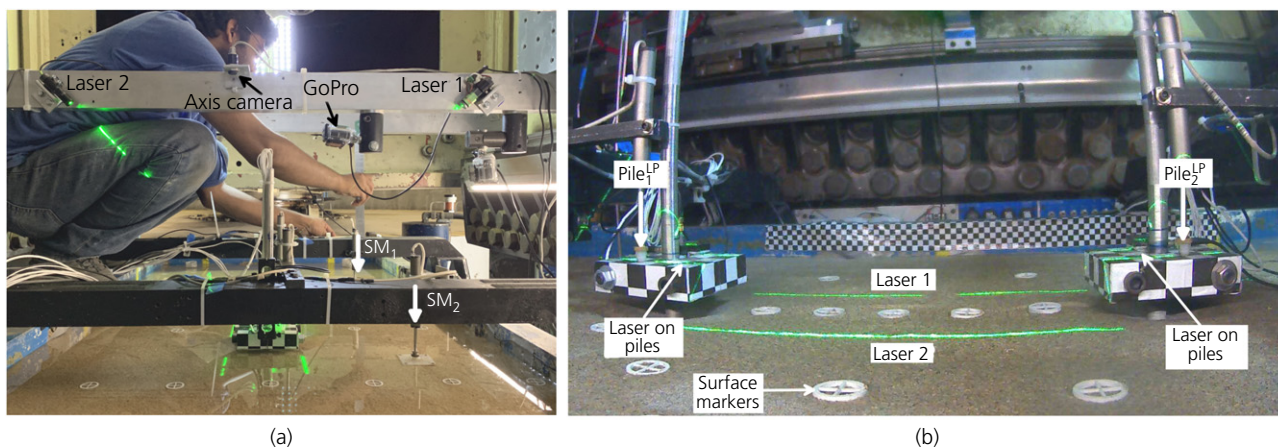
Figure 6. Instrumentation in centrifuge model test SKS02 (Section 3.1): (a) lasers, cameras and soil settlement sensors, (b) surface markers, laser lines and pile settlement sensors

6

International Journal of Physical Modelling in Geotechnics

Measuring vertical displacement using
laser lines and cameras
Sinha, Kutter and Ziotopoulou

(before spinning up and after spin down) were also taken to measure soil settlement.

Two lasers, laser 1 and laser 2, were used to produce laser lines on the soil surface and the pile masses. The lasers were 532 nm, 50 mW green light line lasers bought from Civil Laser (2019). with product IDs 63 and 33 at the time of purchase, respectively. The cost of each laser was about US$60. A cylindrical clamp attached to an angle was used to hold the lasers in place (see Figure 5). Two holes on the angle were made to orient the lasers

with the specified laser angle (θ) while mounting it to the model. The cylindrical clamping mechanism allowed the twisting of the laser to adjust the orientation of the projected laser line. Lasers were installed on either end of the camera beam, projecting laser lines from the east and west side of the model with a laser angle of 46°. The projected laser lines were made parallel to each other, passing through the standing pile mass (see Figure 6(b)). An Axis (P1214-E network) camera with 1280 px × 720 px resolution and 30 frames/s (fps) was installed with its centre facing vertically down at the soil surface. A Hi-speed GoPro (Hero3
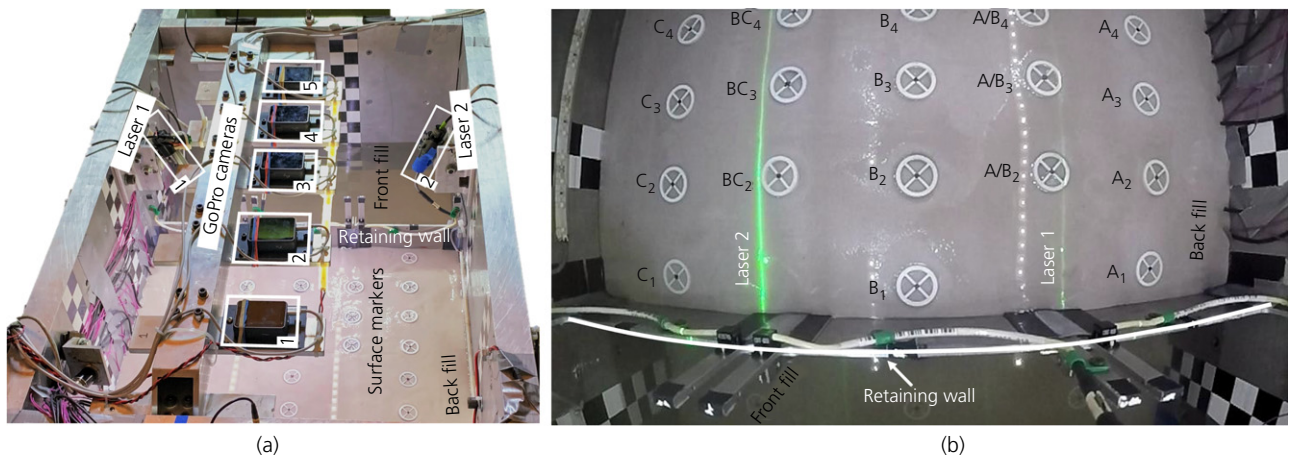

Figure 7. Instrumentation in centrifuge model test BLK01 (Section 3.2). (a) Constructed model showing front and back fill, retaining wall, lasers and cameras. (b) Frame from video recorded by GoPro 3 showing the back fill, retaining wall, surface markers and laser lines
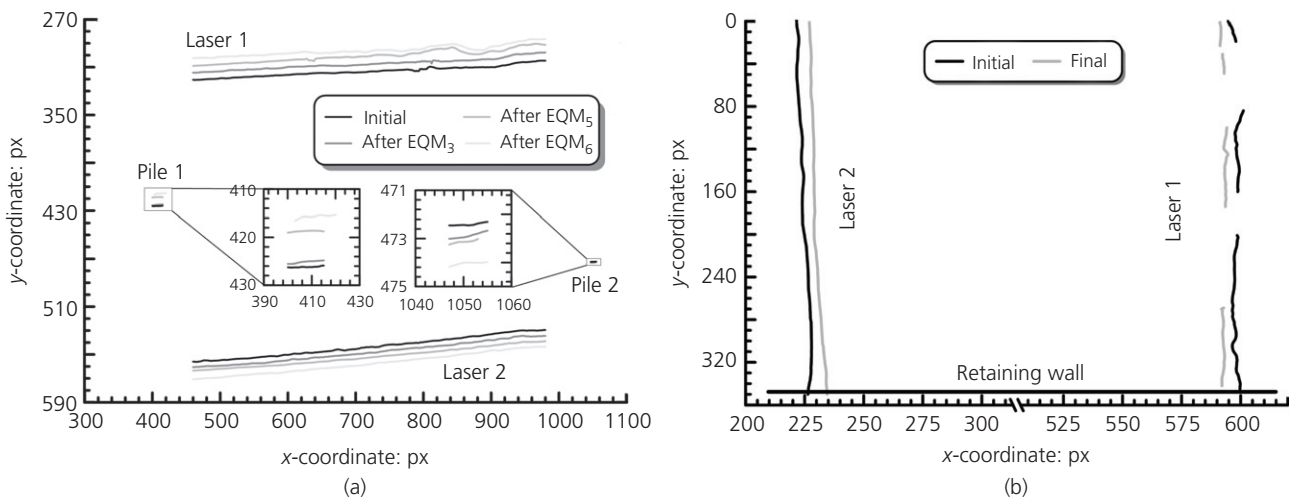

Figure 8. Movement of laser lines after shaking events. (a) Laser line coordinates on soil and pile at the end of shaking events in SKS02 (Section 4.1) centrifuge model test. (b) Initial and final laser line coordinates in BLK01 (Section 4.2) centrifuge model test. Note that the coordinates reported in this figure were obtained after correcting the images for distortion

7

International Journal of Physical Modelling in Geotechnics

Measuring vertical displacement using
laser lines and cameras
Sinha, Kutter and Ziotopoulou

Black Edition) camera with a resolution of 848 px × 480 px of 240 fps was also installed; however, the recorder failed during the test. Surface markers of diameter 25 mm (see Figure 6) were placed between the laser lines (SM_1^{Laser} and SM_2^{Laser}) to find the calibration factor ($f_{px,mm}$) for obtaining soil settlement. Additionally, the pile masses were wrapped with 20 mm × 20 mm grids (see Figure 6) to find the calibration factor ($f_{px,mm}$) around the piles ($Pile_1^{Laser}$ and $Pile_2^{Laser}$) for obtaining pile settlements. The reconsolidation and residual settlements in the soil and the pile computed from processing the laser lines were compared with measurements obtained from the soil and the pile settlement sensors for the major shaking events EQM_3, EQM_5 and EQM_6.

3.2   BLK01 centrifuge test

BLK01 was conducted as part of the liquefaction evaluation and analyses project (LEAP) centrifuge test studying the stability of a liquefiable soil-retaining sheet pile wall (M. Zeghal *et al.*, 2020, personal communication). The backfill consisted of 185.2 mm of medium dense saturated sand ($D_R = 65\%$) extending 475 mm away from the wall, while the front consisted of 74 mm of medium dense saturated sand extending 275 mm from the retaining wall. The model was submerged in water up to the elevation of 185.2 cm. A view of the model is shown in Figure 7(a). The same lasers from the SKS02 test (laser 1 and laser 2) were rigidly mounted on the container's sides, as shown in Figure 7, with laser angles of 67.3 and 66.4°, respectively.
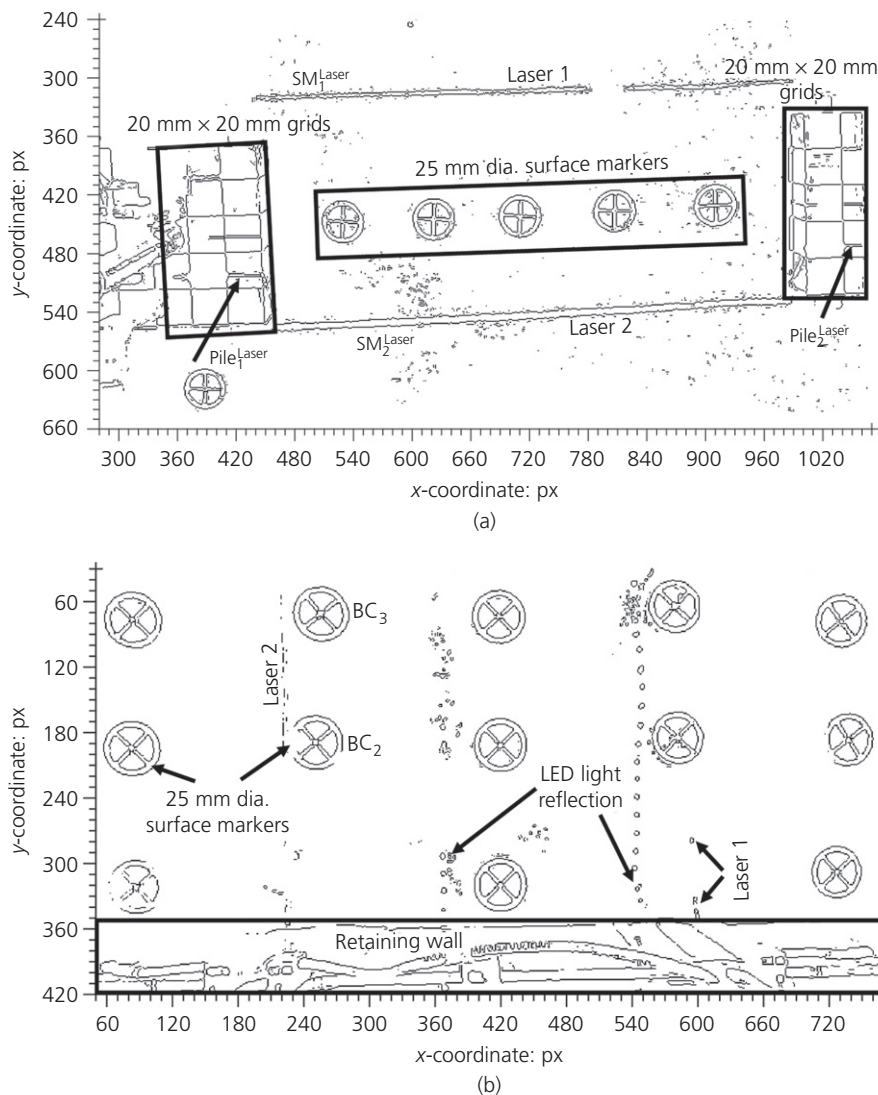

Figure 9. Use of edge detection on images to obtain calibration factor ($f_{px,mm}$) for laser lines on soil and piles using 25 mm dia. surface markers and 20 mm × 20 mm grids in centrifuge model tests (a) SKS02 (Section 4.1) and (b) BLK01 (Section 4.2). LED, light-emitting diode

8

International Journal of Physical Modelling in Geotechnics

Measuring vertical displacement using
laser lines and cameras
Sinha, Kutter and Ziotopoulou

Several surface markers with a diameter of 25 mm were placed on the backfill. Five GoPro Hero5 cameras (numbered as 1, 2, 3, 4 and 5) were installed facing vertically down on the centre-line of the model with overlapping views required for tracking 3D movements of surface markers. The GoPro cameras operated at a frame rate of 240 Hz and recorded images at a resolution of 848 px × 480 px. The model was shaken with 20 cycles of primary 0.037 Hz motion with a 0.1 Hz component, as shown in Figure 12(d). 3D stereophotogrammetry was performed on the recorded images from the overlapping cameras to compute the 3D movements of the surface markers. The

settlements obtained from 3D stereophotogrammetry were then compared with the settlements obtained from analysing the laser line movements in images recorded from camera 3.

4. Results

4.1 SKS02 centrifuge test

Videos recorded from the cameras were processed to obtain displacement−time history plots for the large shaking events EQM_3, EQM_5 and EQM_6. For convenience, the laser lines on pile 1 and pile 2 are correspondingly named $Pile_1^{Laser}$ and
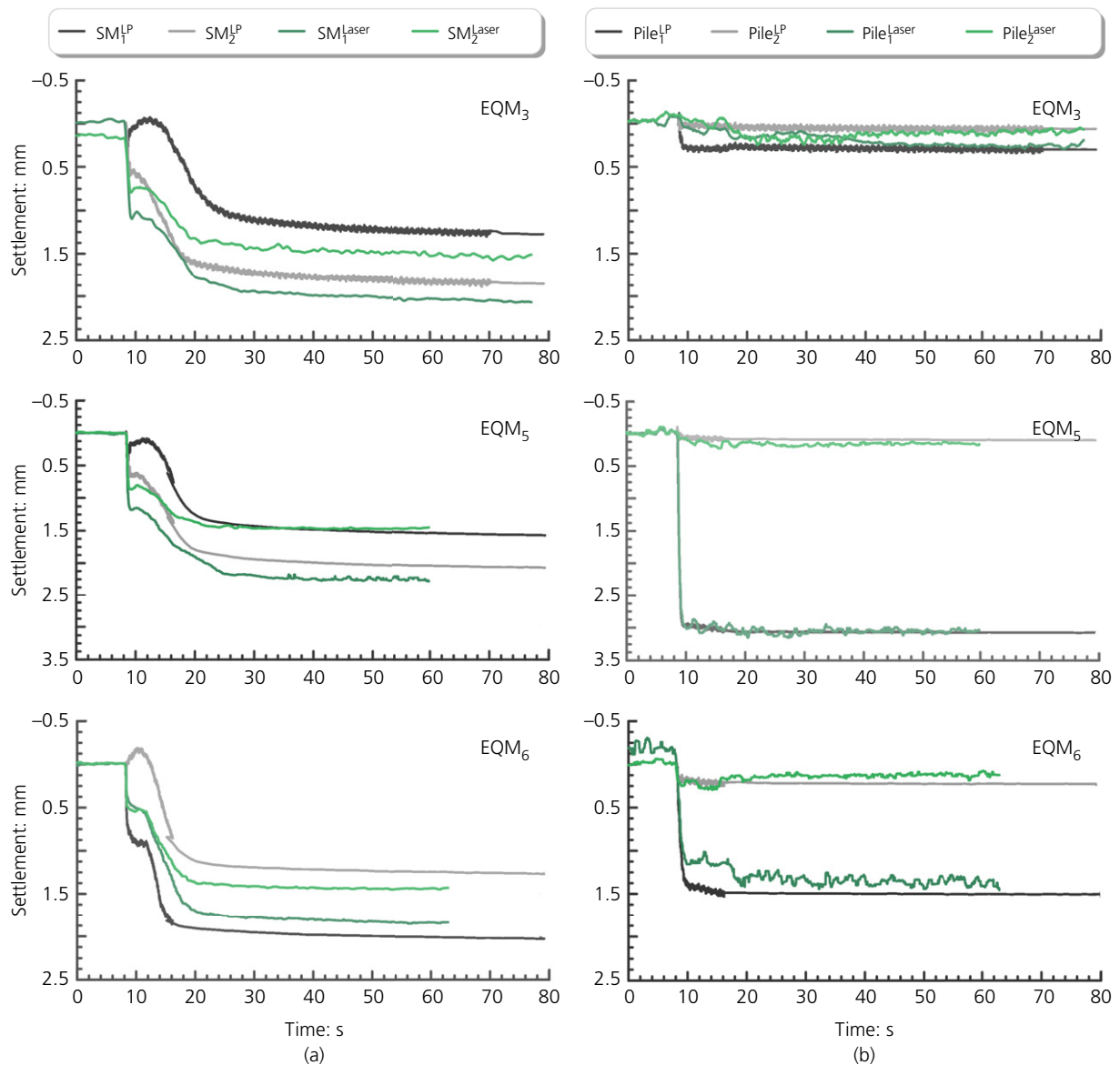

Figure 10. Measured time-histories of (a) soil settlement and (b) pile settlement obtained from lasers and LP sensors for three shaking events: EQM_3, EQM_5 and EQM_6

9

International Journal of Physical Modelling in Geotechnics

Measuring vertical displacement using
laser lines and cameras
Sinha, Kutter and Ziotopoulou

$Pile_2^{Laser}$. Similarly, the laser lines on the soil surface at two distinct locations are named SM_1^{Laser} and SM_2^{Laser}, respectively. Figure 8(a) shows the movements of traced laser lines on soil and pile in image pixel coordinates at the end of shaking events EQM_3, EQM_5 and EQM_6. With multiple shakings, the laser lines moved away from each other. The magnitude of movement provides an indication of liquefaction-induced soil settlement. Videos recorded from high-resolution axis cameras were processed to obtain dynamic vertical movements in soil and pile. Figure 9 shows the edges of laser lines ($Pile_1^{Laser}$, $Pile_2^{Laser}$, SM_1^{Laser} and SM_2^{Laser}) and the piles produced from the edge detection algorithm applied on a recorded video frame. Edge detection on the video frames (see Figure 9) was used to measure the dimensions of the known 25 mm dia. soil surface markers and 20 mm × 20 mm grid in pixels. The 25 mm dia. soil surface marker in the image (see Figure 9(a)) occupied 29 pixels resulting in the calibration factor $f_{px,mm}$ of 1.16 px/mm for the laser lines located on the soil surface. Similarly, the 20 mm square grid in the image occupied 25 pixels resulting in the calibration factor $f_{px,mm}$ of 1.25 px/mm for the laser lines located on the piles. Note that the difference in the calibration factors ($f_{px,mm}$) for laser lines on the soil and on the piles arises from the difference in magnification of different points in the image. With the piles being 40 mm higher in elevation than the soil, they were also closer to the camera, resulting in a greater magnification and thus a larger calibration factor ($f_{px,mm}$). In this case and for all shaking events, the settlement of the targets was small and therefore did not affect the initial calibration factor ($f_{px,mm}$). Using a smooth spline interpolation (Figure 4(a)), the laser lines were traced with a subpixel accuracy of 0.1 px. With the subpixel resolution of 0.1 px, the computed horizontal movements (u_c) of laser lines on soil and pile produced an accuracy of ± 0.09 and ± 0.08 mm, respectively. The camera recording frequency of 30 Hz was not insufficient to capture dynamic movements during shaking, but it was able to capture the reconsolidation settlements (see Section 4.1.1).

The camera angles for SM_1^{Laser} and SM_2^{Laser} were about 4.8 and 10°, respectively. While the centre of the camera image was pointing perpendicular to the soil surface, the camera angles (θ) varied with distance from the centre of the image. The camera angle for $Pile_1^{Laser}$ and $Pile_2^{Laser}$ laser lines was found to be about 4.2°. With subpixel resolution of 0.1 px, the computed vertical settlement in the soil and pile settlement produced an accuracy of about ± 0.09 mm. The accuracy of the settlement measured could be increased by using sharper laser lines, higher resolution cameras, or by moving the camera closer to the target. The accuracy of the settlement sensors was measured to be about ± 0.1 mm. Pile settlements obtained from $Pile_1^{Laser}$ and $Pile_2^{Laser}$ were compared with the measured settlements from $Pile_1^{LP}$ and $Pile_2^{LP}$, respectively. Similarly, soil settlements obtained from SM_1^{Laser} and SM_2^{Laser} were compared with SM_1^{LP} and SM_2^{LP}, respectively. Soil settlements from the laser lines were obtained by averaging the settlements over the length of 150 mm at the centre of the laser line. It should be noted that in both the studies presented in this paper, the soil surface was initially not submerged in water. Only after shaking when the soil had reconsolidated, a small amount of water came to the surface. The depth of water above the surface had minimal effect on the results presented in this paper.
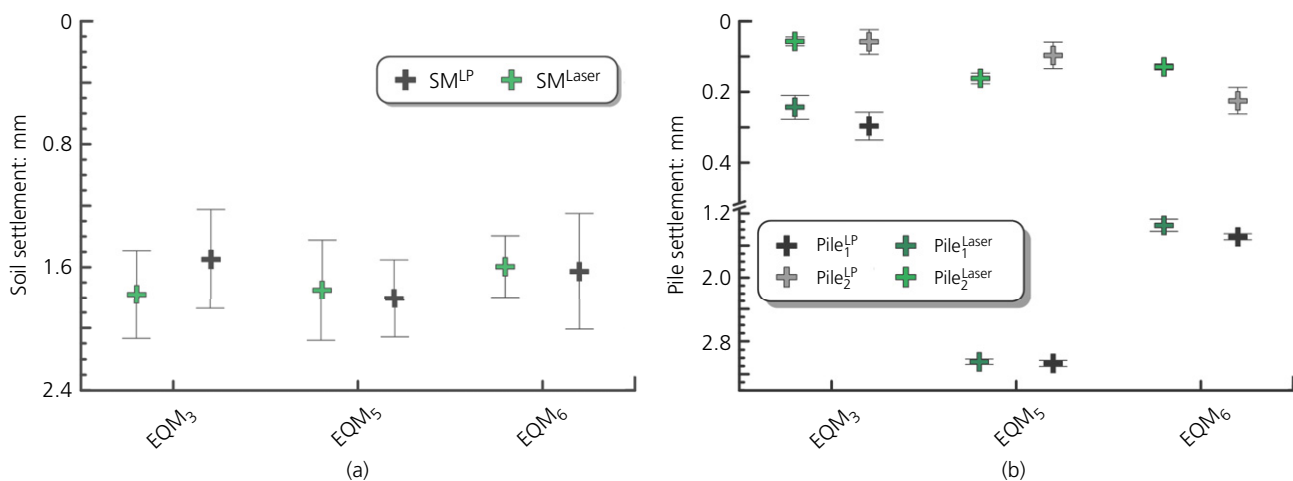

Figure 11. Comparison of (a) soil settlement and (b) pile settlement obtained from lasers with settlements measurements from LPs for different shaking events in SKS02 (Section 4.1) centrifuge test

International Journal of Physical Modelling in Geotechnics

Measuring vertical displacement using
laser lines and cameras
Sinha, Kutter and Ziotopoulou

4.1.1 Reconsolidation settlements

Figure 10 plots the settlement in the soil and the pile for three shaking events EQM_3, EQM_5 and EQM_6. It can be observed that the settlement histories obtained from laser lines match quite well with the recorded measurements from settlement sensors. Since SM_1^{Laser}, SM_2^{Laser}, SM_1^{LP} and SM_2^{LP} physically measured soil settlement at distinct locations, they were expected to differ from the surface settlement variation. SM_1^{Laser} and SM_2^{Laser} were able to match all the features of the soil settlement response. The obtained response showed a quick drop in the settlement at the end of shaking, followed by a constant settlement (with a slight upward movement) for about 3 s and then slow reconsolidation of the soil. It perfectly matched the initial sudden drop in settlement at the end of the shaking, followed by less than 0.2 mm settlement during reconsolidation. The rate of the reconsolidation settlement was found to be very similar for both SM^{Laser} and SM^{LP}. Pile settlements $Pile_1^{Laser}$, $Pile_2^{Laser}$ obtained from laser lines matched quite well with the pile settlement sensors $Pile_1^{LP}$ and $Pile_2^{LP}$, respectively.

4.1.2 Residual settlements

Figure 11 plots the residual settlement in soil and pile (with a 95% confidence interval) obtained at the end of the reconsolidation ($t = 80$ s). The soil settlement recorded from linear displacement sensors and laser lines varied by ± 0.4 mm. The variations could have resulted from the non-uniform settlement of the soil surface. However, a very tiny variation ($< \approx \pm 0.1$ mm) was observed for pile settlements. The settlements obtained from the laser lines agreed quite well within the 95% confidence interval with an accuracy of about ± 0.10 mm.

4.2 BLK01 centrifuge test

The recordings obtained from the GoPro cameras were first processed to remove distortions. Figure 7 and Figure 4(b) show the distorted and undistorted frame for GoPro camera 3. The undistorted image was then processed to trace the laser lines. Figure 8(b) shows the movements of traced laser lines in image pixel coordinates before and after the shaking event. Using edge detection on the recorded images with surface markers of diameter 25 mm (see Figure 9(b)), the calibration factor ($f_{px,mm}$) of 1.942 and 2 px/mm were obtained for laser 1 and laser 2, respectively. The camera view angles for the laser lines were measured to be 23.43 and 24.50°, respectively. With subpixel resolution of 0.1 px, the accuracy in vertical settlement measured by laser 1 and laser 2 came to be ± 0.05 and ± 0.06 mm, respectively; 240 fps provided good resolution in time to capture the frequency content of the motion. Sections 4.2.1 and 4.2.2 compare the soil settlement obtained from the processing of laser lines with the results from 3D stereophotogrammetry performed in TEMA software (ISMA, 2019).

4.2.1 Dynamic settlements

Figure 12 plots the soil settlement at $x = 5$ mm, $x = 87$ mm and $x = 137$ mm away from the retaining wall during the applied shaking motion. The settlements of the surface markers BC_3 and BC_2 were obtained from 3D
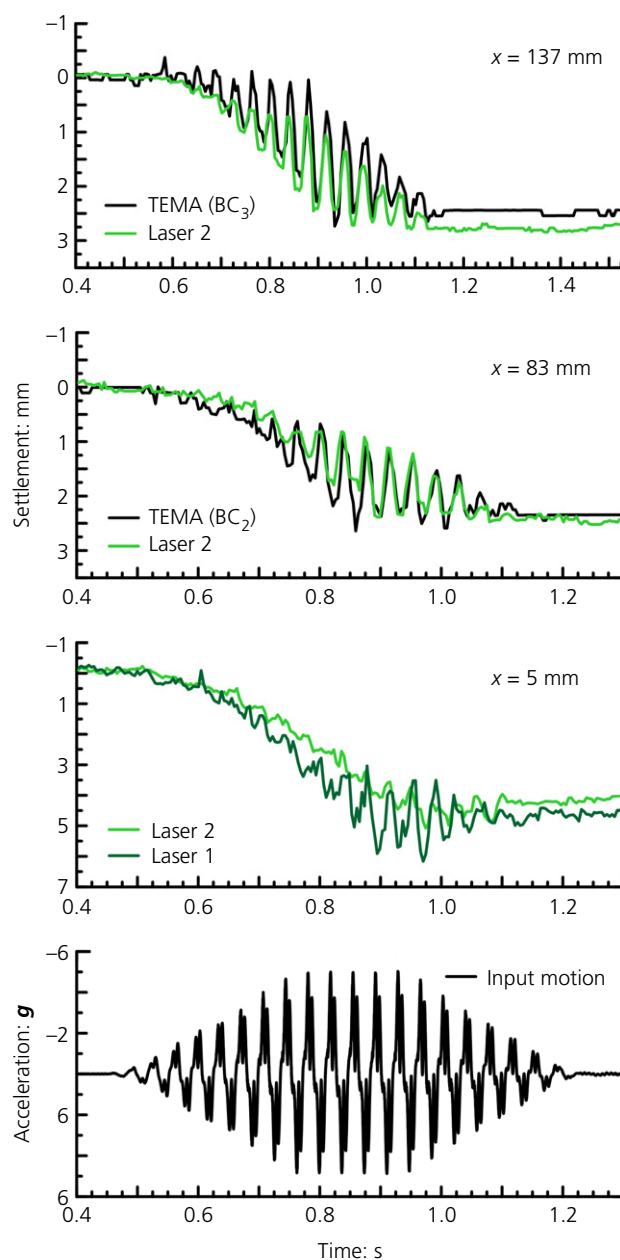

Figure 12. Comparison of dynamic soil movement at $x = 5$ mm, $x = 83$ mm and $x = 137$ mm away from the retaining wall, obtained from lasers with the movements obtained from 3D stereophotogrammetry on nearest surface markers during shaking in BLK01 (Section 4.2) centrifuge model test
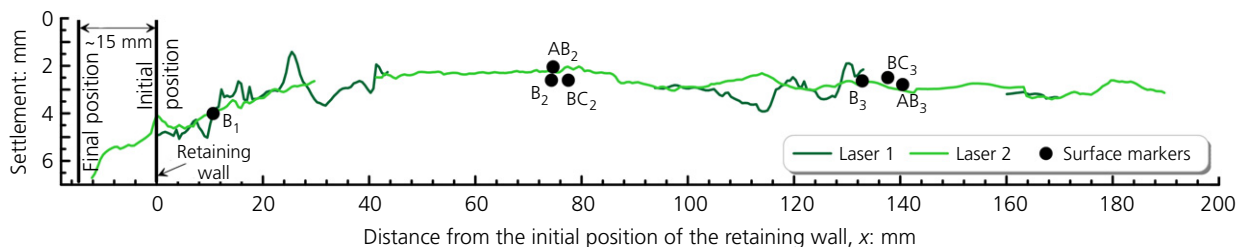
11

Figure 13. Soil settlement profile (vertical exaggeration of ∼28×) away from the retaining wall at the end of motion (after 14.6 s) in BLK01 (Section 4.2) centrifuge model test

stereophotogrammetry performed in TEMA. The laser lines closest to the surface markers (BC_2, BC_3) were used to compare the settlements obtained from TEMA. Laser line 2 near the surface marker BC_4 and laser line 1 near the surface marker A/B_2, A/B_3 and A/B_4 could not be appropriately traced due to their low intensity and interference from the movement of the surface markers during shaking. However, near the retaining wall, where there was no such hindrance, settlements were evaluated for laser line 1 and laser line 2, as shown in Figure 12. From the figure, it can be observed that the processed settlements from the laser lines clearly pick up the frequency of the motion and match quite well with the settlements obtained from 3D stereophotogrammetry analysis. While the methods compared in Figure 12 provide excellent agreement with respect to the measured residual displacements, there is noticeable discrepancy with respect to the amplitude of cyclic displacements. This difference could have resulted from the real variability in the soil response, disturbance produced from the surface marker on the soil nearby, and/or from the discrepancies between one of the two methods.

4.2.2 Residual settlements

Figure 13 plots the residual soil settlement profile away from the retaining wall. The settlement profile is shown 14.6 s after the end of the motion. Settlements obtained from 3D stereophotogrammetry on surface markers are also shown in the figure. At the end of the shake, the wall rotated and moved about 15 mm laterally at the backfill elevation. About 7 mm of soil settlement occurred near the retaining wall. Away from the retaining wall, the settlement gradually decreased. About 100 mm apart, the settlement remained constant at about 3 mm. A small upheave observed between 40 and 80 mm away from the retaining wall agreed well with the post-excavation survey conducted on the settled soil surface. From the results shown in Figure 13, it can be observed that the settlements evaluated from the laser lines agree quite well with the settlements obtained at surface marker location by 3D stereophotogrammetry.

5. Conclusions

A new method using lasers and a camera was developed to track dynamic and residual vertical movements in model tests. The method works by video recording the projected laser lines on the test object. The video is then processed to track horizontal movements of laser lines in pixels in time. Pixel movements are then used to obtain vertical movements using an image calibration factor ($f_{px,mm}$), the camera angle (ϕ), the laser angle (θ) and the slope of the settled surface (α). The new method was used in two centrifuge model tests, and the results were presented. The accuracy of the measurements produced in these tests were in the range of 0.05–0.1 mm. The method was validated by comparing the results to those obtained by hand measurement, LPs and 3D stereophotogrammetry performed in TEMA software. This paper explains the techniques developed for practical implementation in a centrifuge model test.

This new method overcomes the limitations of the traditional contact-based settlement sensors. Having no physical contact eliminates the concern of changing the structural response and introducing spurious vibrations. It also exposes the model surface for image analysis and makes it available for performing other important investigations. With a single laser and a single camera, this method can trace the movements of multiple targets that the laser line crosses, which can significantly help in reducing the sensor requirements and the associated expenses of a model test. The method offers flexibility in choosing the laser's position and the camera angle, making their placement easier in the model, avoiding congestion. The method provides spatially and temporally continuous settlement data along the laser line and produces accuracy similar to DIC and PIV methods. The technique used for computing settlements from the video recordings of laser lines is simpler, faster and cheaper than DIC and PIV methods. However, for cases where the entire model needs to be monitored for movements, DIC and PIV methods may be preferred. With the development of new high-definition and high-frequency cameras and the advances in image processing techniques, the new method is a step further in the direction of the future of model tests with non-contact sensors.

12

International Journal of Physical Modelling in Geotechnics

Measuring vertical displacement using
laser lines and cameras
Sinha, Kutter and Ziotopoulou

Data Availability Statement

Some or all the data (sample images and recordings used for the procedure) are available from the corresponding author by request.

REFERENCES

Adrian RJ (1991) Particle-imaging techniques for experimental fluid mechanics. *Annual Review of Fluid Mechanics* **23(1)**: 261–304.

Carey T, Stone N and Kutter BL (2018) A new procedure for tracking displacements of submerged sloping ground in centrifuge testing. In *Physical Modelling in Geotechnics – ICPMG 2018* (McNamara A, Divall S, Goodey R, Taylor N, Stallebrass S and Panchal J (eds)). CRC Press, London, UK, pp. 829–834.

Civil Laser (2019) *Green Laser Module Line (Laser Head)*. NaKu Technology Co., Ltd, Hangzhou, China. See https://www.civillaser.com/ (accessed 04/11/2021).

Farrell RP (2010) *Tunnelling in Sands and the Response of Buildings*. Doctoral dissertation, University of Cambridge, Cambridge, UK.

Fiegel BGL and Kutter BL (1994) Liquefaction mechanism for layered sands. *Journal of Geotechnical Engineering* **120(4)**: 737–755.

Gerber E (1929) *Untersuchungen über die Druckverteilung im örtlich belasteten Sand*. Doctoral dissertation, ETH Zurich, Zurich, Switzerland (in German).

IDICS (International Digital Image Correlation Society), Jones EMC and Iadicola MA (eds) (2018) *A Good Practices Guide for Digital Image Correlation*. IDICS, Gaithersburg, MD, USA, https://doi.org/10.32720/idics/gpg.ed1.

ISMA (Image Systems Motion Analysis) (2019) *TEMA Classic 3D*, Version 2019c. ISMA. Linköping, Sweden. See http://www.imagesystems.se/ (accessed 04/11/2021).

James RG (1965) *Stress and Strain Fields in Sand*. Doctoral dissertation, University of Cambridge, Cambridge, UK.

Kutter BL and Balakrishnan A (1998) Dynamic model test data from electronics to knowledge. In *Centrifuge '98* (Kimura T, Kusakabe O and Takemura J (eds)). Balkema, Rotterdam, the Netherlands, vol. 2, pp. 931–943.

Ritter S (2017) *Experiments in Tunnel-Soil-Structure Interaction*. Doctoral dissertation, University of Cambridge, Cambridge, UK.

Sinha SK, Ziotopoulou K and Kutter BL (2021a) *Centrifuge Testing of Liquefaction-Induced Downdrag on Axially Loaded Piles: Data Report for SKS02*. Center for Geotechnical Modeling, University of California Davis, Davis, CA, USA, Report no. UCD/CGMDR – 21/01.

Sinha SK, Ziotopoulou K and Kutter BL (2021b) *Centrifuge Testing of Liquefaction-Induced Downdrag on Axially Loaded Piles: Data Report for SKS03*. Center for Geotechnical Modeling, University of California Davis, Davis, CA, USA, Report no. UCD/CGMDR – 21/02.

Sinha SK, Kutter BL, Wilson D, Carey T and Ziotopoulou K (2021c) *Use of Photron Cameras and TEMA Software to Measure 3D Displacements in Centrifuge Tests*. Center for Geotechnical Modeling, University of California Davis, Davis, CA, USA, Report no. UCD/CGM – 21/01.

White D, Take A and Bolton M (2001) Measuring soil deformation in geotechnical models using digital images and PIV analysis. In *Computer Methods and Advances in Geomechanics* (Desai CS, Kundu T, Harpalani S, Contractor D and Kemeny J (eds)). CRC Press/Balkema, Rotterdam, the Netherlands, pp. 997–1002.

How can you contribute?

To discuss this paper, please email up to 500 words to the editor at journals@ice.org.uk. Your contribution will be forwarded to the author(s) for a reply and, if considered appropriate by the editorial board, it will be published as discussion in a future issue of the journal.

International Journal of Physical Modelling in Geotechnics relies entirely on contributions from the civil engineering profession (and allied disciplines). Information about how to submit your paper online is available at www.icevirtuallibrary.com/page/authors, where you will also find detailed author guidelines.